Electronic Supplementary Material (ESI) for Materials Chemistry Frontiers.

Supporting Information

Synthesis and Post-Polymerization Functionalization of a Tosylated Hyper-Crosslinked Polymer for Fast and Efficient Removal of Organic Pollutants in Water

Bunyaporn Todee,[a] Threeraphat Chutimasakul,[b] Kritanan Junthod,[a] Andrew Docker,[c] Phoonthawee Saetear,[a] Manisa Kongkaew,[d] Thachanok Ratvijitvech,[a] Jonggol Tantirungrotechai,[a] Thanthapatra Bunchuay [a*]

[a] *Department of Chemistry, Faculty of Science, Mahidol University, Rama VI Rd, Bangkok 10400, Thailand.*
[b] *Thailand Institute of Nuclear Technology (Public Organization), 9/9 moo 7, Saimoon Ongkharak District, Nakhon Nayok 26120, Thailand.*
[c] Department of Chemistry, University of Oxford Chemistry Research Laboratory Mansfield Road, Oxford OX1 3TA
[d] *Department of Science and Technology, Faculty of Science, Pibulsongkram Rajabhat University, Phlai Chumphon, Mueang Phitsanulok District, Phitsanulok 65000, Thailand.*

Table of Contents

Experimental Methods

1. Synthesis

1.1 Synthesis of M-OTs precursor

A solution of 1,4-bis(2-hydroxyethoxy)benzene (11.5 g, 58.0 mmol) in THF (150 mL) was mixed with an aqueous solution of NaOH (14 g, 350 mmol in water 20 mL) at 0 °C, follow by portionwise addition of solution of p-toluenesulfonyl chloride (25 g, 130 mmol). The mixture of solution was stirred at r.t. for 2 hours, the organic solvent was removed *in vacuo*. The mixture was poured into ice water, the white precipitate formed was collected by filtration and washed several times with a large volume of water (ca. 500 ml). The crude product was further purified by soaking in ethanol at 0 °C overnight and filtered to afford a white-colored solid. The solid product was washed with a large volume of methanol (ca. 500 ml), which gave 25.1 g of the desired monomer M-OTs (85%)

1.2 Synthesis of P-OTs

A 50-mL round bottom flask was charged with **M-OTs** (4.05 g, 8.00 mmol), dimethoxymethane (1.22 g, 16.00 mmol), and 1,2-dichloethane (16 mL). Anhydrous $FeCl_3$ (2.60 g, 16.00 mmol) was added portionwise over 5 minutes, and the mixture was then stirred at 80 °C. After 18 h, the obtained blackish polymer was poured into MeOH (30 mL) and the solid residue was collected by filtration, which was subsequently purified by Soxhlet extraction using MeOH for 24 h, and dried under vacuum at r.t. for 48 h. **P-OTs** was obtained as black solid (4.08 g, 7.85 mmol, 98%).

1.3 Synthesis of sulfonated HCPs (P-SO_3H)

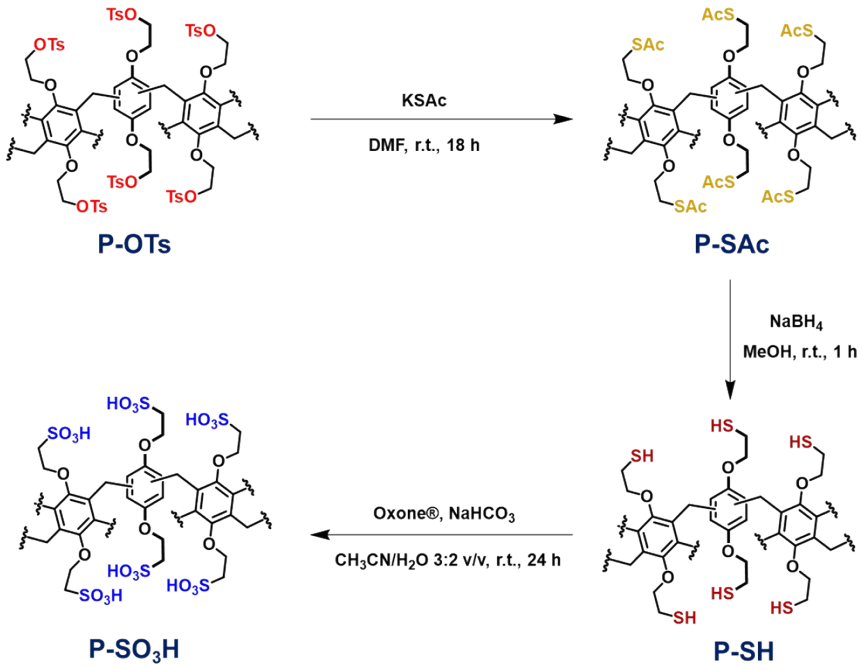

Figure S1 Synthesis of sulfonated HCPs by post-polymerization methods.

1.4 Synthesis of a sulfur-free HCP (P-OEt)

A fine powder of 1,4-diethoxybenzene (0.6649 g, 4 mmol) was dissolved with 1,2-dichloethane (6 mL). Dimethoxymethane (0.61 g, 8 mmol) and $FeCl_3$ (1.30 g, mmol) were added to the mixture solution. After refluxed overnight, the reaction mixture was poured into methanol and the blackish precipitate was filtered and collected only the solid residue. The product was then purified by Soxhlet in methanol overnight and dried under vacuum at r.t. for 48 h to afford the target product **P-OEt** (0.59 g, 3.28 mmol, 82%).

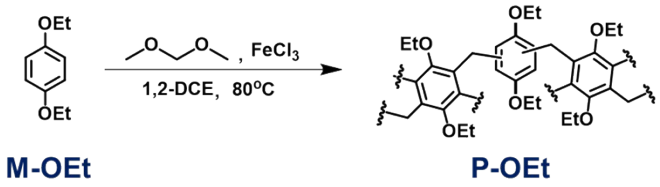

Figure S2 Synthesis of **P-OEt.**

2. Adsorption studies

2.1 Static adsorption experiment of organic dyes

Static adsorption experiments of all synthesized polymers were carried out with both cationic dyes (Methylene blue, **MB**; Methyl violet, **MV**; Rhodamine B; **RB**) and the anionic dye (Methyl orange; **MO**). A solution of dye (100 ppm, 20 mL) was added to a sample of polymer (20 mg) and stirred at room temperature for 24 hours. The suspension was subsequently filtered through a syringe filter to remove the polymer solid. The amount of dye remaining in the filtered solution was determined by UV-visible spectrophotometry, recording the intensity of absorption at the wavelength of maximum of absorption of each dye; **MB** (664 nm), **MV** (594 nm), **RB** (554 nm), and **MO** (464 nm).

2.2 Static adsorption experiment of paraquat (PQ)

Adsorption experiments of **PQ** followed the same procedure for the adsorption of dyes. Due to the colourless nature of **PQ**, addition of a 1% (w/v) sodium dithionite in 0.06 mM NaOH was required to develop a blue solution for determination of **PQ** by spectrophotometry at its maximum absorption wavelength (603 nm).[1]

2.3 Kinetic adsorption experiment

An aqueous solution of organic pollutants (20 ml) with initial concentrations of either C_i =200, 300, and 400 ppm for **MB**, and C_i = 100, 150, and 200 ppm for **PQ** was added to **P-SO_3H** (20 mg) and stirred at 350 rpm at room temperature. Aliquots of solution were removed at given time intervals and taken for analysis by recording the UV-visible spectrum at 664 nm (**MB**) and 603 nm (**PQ**). Analysis of **MB** and **PQ** followed the typical procedures reported above.

2.4 Isotherm adsorption experiment

An aqueous solution of organic pollutants (20 ml) with initial concentration (C_i = 100-600 ppm for **MB**, and C_i = 50-1000 ppm for **PQ**) was added **P-SO_3H** (20 mg) and stirred at 350 rpm at room temperature for 2 h. The solution was taken for analysis of a target analyte by UV-visible spectrophotometer at 664 nm (**MB**) and 603 nm (**PQ**). Analysis of **MB** and **PQ** followed the typical procedures reported above.

2.5 Effect of pH

The effect of pH on adsorption performance was studied in phosphate buffers at pH values including 6, 7, and 9 to represent the acidic, neutral, and basic solution conditions. Adsorption experiments and analysis were carried out as the typical procedure in 2.1.

2.6 Effect of ionic strength

In this study, stock solutions of sea water and fresh water were prepared followed the literature procedure, these stock solutions were used to prepare a solution of **MB** (20 mL, 400 ppm) to which **P-SO_3H** (20 mg) was added and stirred for 24 h. A clear solution of remaining **MB** was monitored by UV-visible analysis (at wavelength 664 nm). Adsorption of **PQ** followed the same method for **MB**, but the initial concentration of **PQ** was 200 ppm. The remaining **PQ** solution after adsorption was treated with a 1% solution (w/v) of sodium dithionite before monitoring by UV-visible analysis (at wavelength 603 nm).

2.7 Dye mixture adsorption experiments

An aqueous solution of a cationic dye (10 mL, 100 ppm) was mixed with an aqueous solution of an anionic dye (10 mL, 100 ppm), then the mixture was treated with 20 mg of **P-SO_3H** and stirred for 24 h at 350 rpm at r.t. After which, **P-SO_3H** was removed from the solution by filtration, and the remaining dye in solution was subsequently measured using a UV-visible spectrophotometer.

Characterization

1. FTIR peak assignments of monomer and polymers.

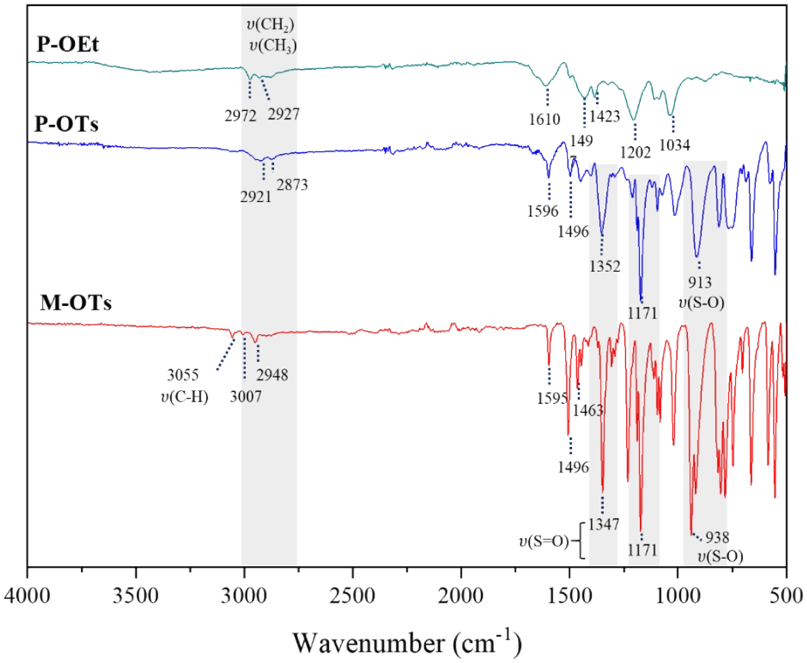

Figure S3 FTIR spectra of the **M-OTs** and its corresponding polymer (**P-OTs**) comparing with the sulfur-free HCP (**P-OEt**).

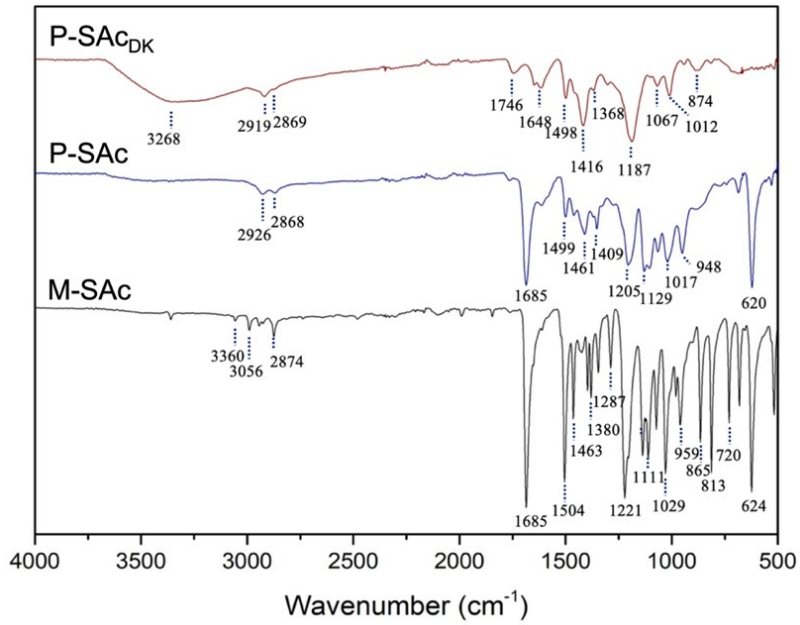

Figuer S4 IR spectra of the **M-SAc** and the corresponding polymer (**P-SAc$_{DK}$**) synthesized by direct knitting comparing with **P-SAc** synthesized via the post-psynthetic modification of **P-OTs**.

Table S1 FTIR peak assignments of **M-OTs**, **P-OTs**, **P-SAc**, **P-SH**, **P-SO_3H**

M-OTs	Vibrational mode	P-OTs	Vibrational mode	P-SAc	Vibrational mode	P-SH	Vibrational mode	P-SO_3H	Vibrational mode
3055	ν(C-H), w							3417	ν(O-H), m
3007	$\nu(CH_2)$, $\nu(CH_3)$, w								
2948	$\nu(CH_2)$, $\nu(CH_3)$, w	2912	$\nu(CH_2)$, $\nu(CH_3)$, w	2926	$\nu(CH_2)$, $\nu(CH_3)$, w	2924	$\nu(CH_2)$, $\nu(CH_3)$, w	2930	$\nu(CH_2)$, $\nu(CH_3)$, w
		2873	$\nu(CH_2)$, $\nu(CH_3)$, w	2868	$\nu(CH_2)$, $\nu(CH_3)$, w	2870	$\nu(CH_2)$, $\nu(CH_3)$, w		
				1685	ν(C=O), vs			1681	ν(C=C), m
1595	ν(C=C), m	1596	ν(C=C), m	1612	ν(C=C), w	1612	ν(C=C), w	1622	ν(C=C), m
1506	ν(C=C), s	1496	ν(C=C), m	1499	ν(C=C), w	1500	ν(C=C), w	1501	ν(C=C), w
1463	$\delta(CH_2)$, m	1448	$\delta(CH_2)$, m	1461	$\delta(CH_2)$, m	1460	$\delta(CH_2)$, m	1455	$\delta(CH_2)$, m
1445	$\delta(CH_2)$, m	1400	$\delta(CH_3)$, m	1409	$\delta(CH_3)$, w	1408	$\delta(CH_3)$, w	1412	$\delta(CH_3)$, w
1413	$\delta(CH_3)$, w			1352	$\delta(CH_2)$, m	1369	$\delta(CH_2)$, m	1372	$\delta(CH_2)$, m
1347	Sulfonate, ν(S=O), vs	1352	Sulfonate, ν(S=O), s						
1231	$\delta(CH_2)$, m	1210	$\delta(CH_2)$, m	1205	$\delta(CH_2)$, m	1202	$\delta(CH_2)$, m		
1171	Sulfonate, ν(S=O), vs	1171	Sulfonate, ν(S=O), vs					1172	ν(S=O), vs
1020	ν(C-O), s	1016	ν(C-O), s	1129	ν(C-O), s	1010	ν(C-O), s	1037	ν(C-O), s
938	Sulfonate, ν(S-O), vs	913	Sulfonate, ν(S-O), vs	620	δ(C-S), s	685	ν(C-S), w/ ν(S-S), w		

2. Elemental analysis

Table S2 The elemental analysis of monomer and sulfur-containing polymers.

Network	%C	%H	%S
M-OTs (actual)	75.84 ± 3.40	6.52 ± 0.07	10.04 ± 0.79
M-OTs (calc.)	56.90	5.17	12.66
P-OTs (actual)	72.15 ± 13.10	5.53 ± 0.68	8.10 ± 0.77
P-OTs (calc.)	57.79	5.24	12.34
P-SAc (actual)	87.67 ± 1.89	6.9329 ± 0.186	12.52 ± 1.53
P-SAc (calc.)	55.02	5.85	19.58
P-SH (actual)	64.01 ± 8.11	5.05 ± 0.04	11.97 ± 0.14
P-SH (calc.)	54.29	6.21	26.35
P-SO_3H (actual)	48.58 ± 0.10	4.45 ± 0.27	12.73 ± 0.04
P-SO_3H (calc.)	38.93	4.46	18.89
P-OEt (actual)	72.27 ± 0.11	5.75 ± 0.02	-
P-OEt (calc.)	73.71	8.44	-

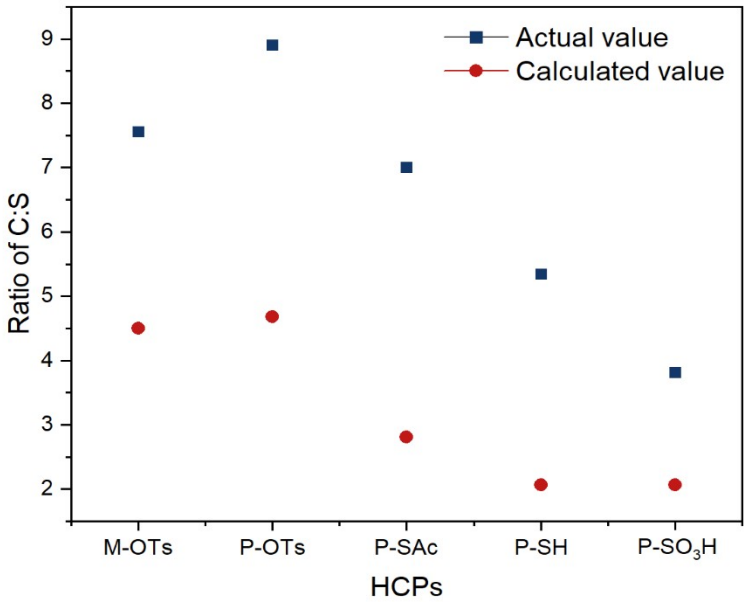

Figure S5 Trend of C:S ratio of sulphur-containing HCPs after post functionalisation.

3. Thermal analysis

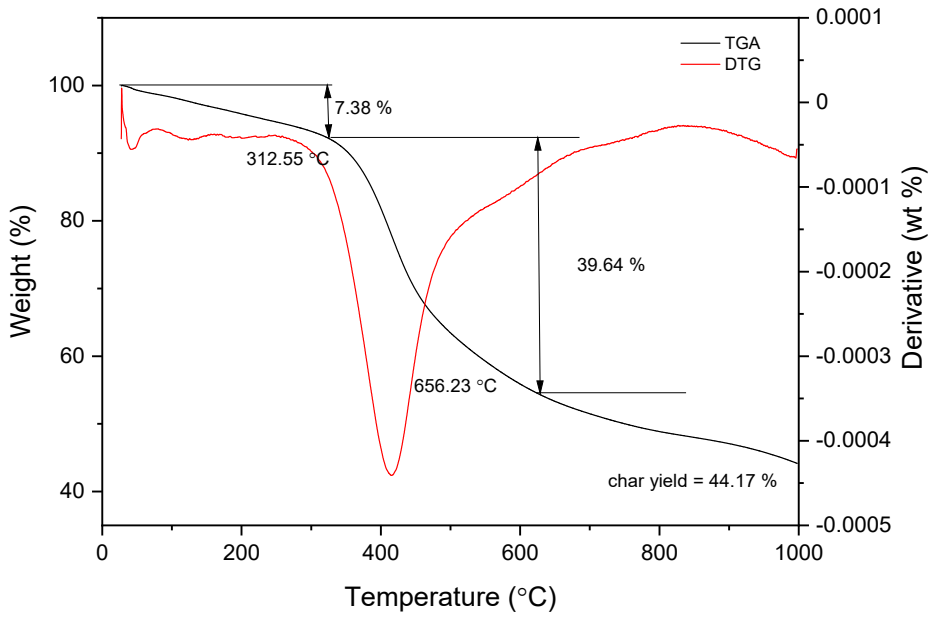

Figure S6 Thermogravimetric analysis (TGA) thermograms of the **P-OEt**.

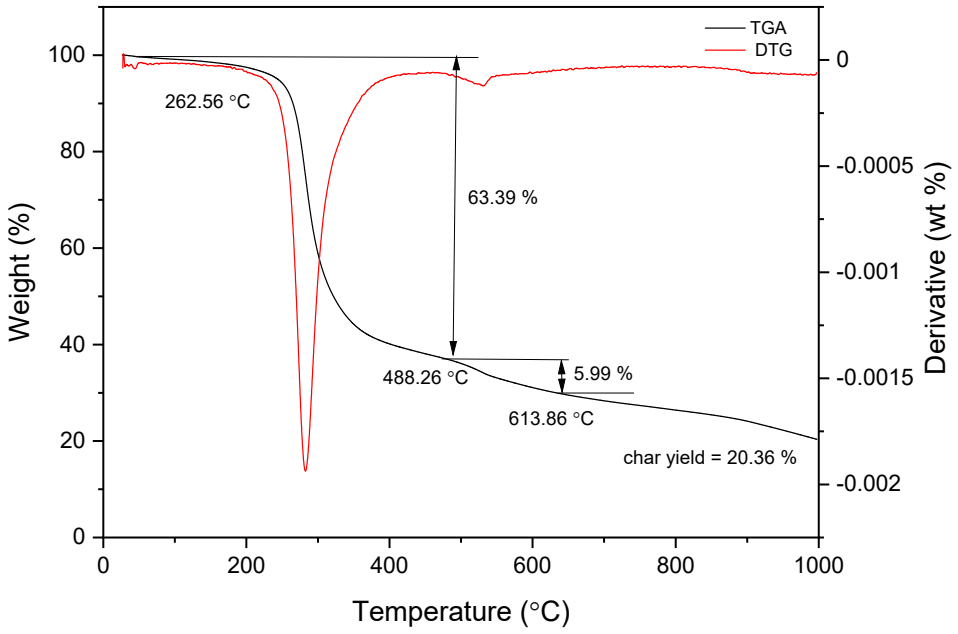

Figure S7 Thermogravimetric analysis (TGA) thermograms of the **P-OTs**.

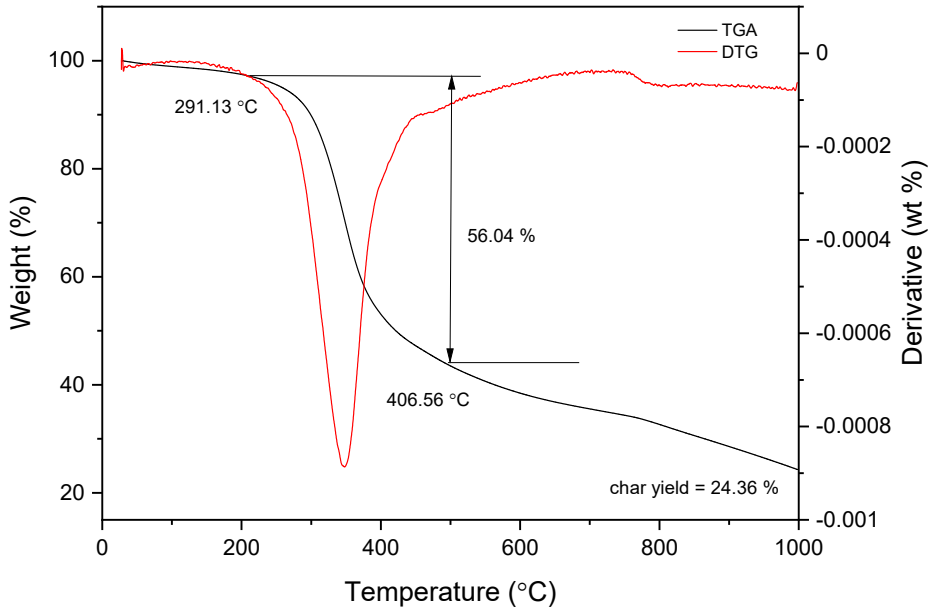

Figure S8 Thermogravimetric analysis (TGA) thermograms of **P-SAc**.

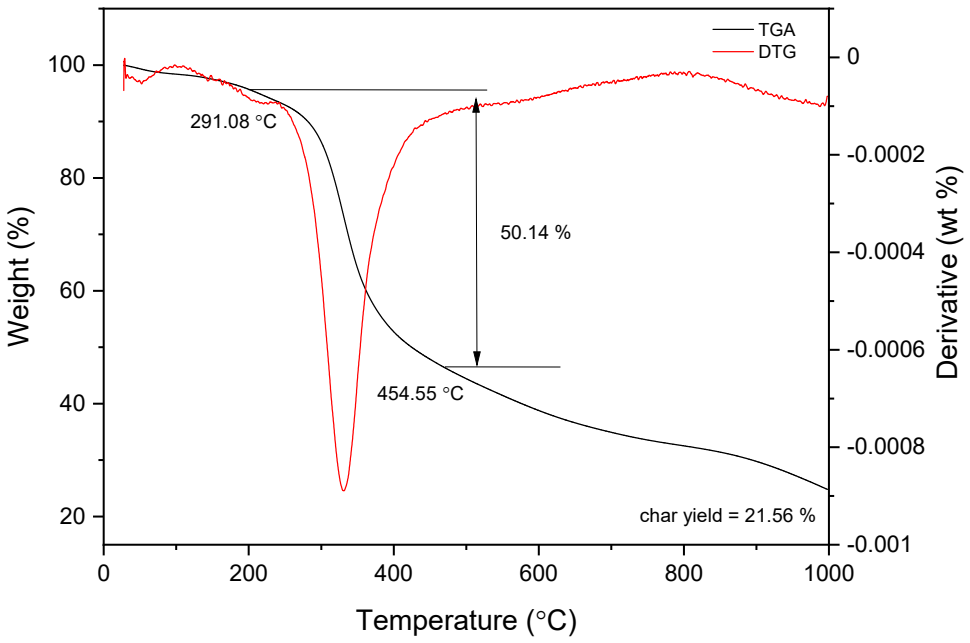

Figure S9 Thermogravimetric analysis (TGA) thermograms of **P-SH**.

Table S3 Weight loss in temperature ranges of the synthesized HCPs.

HCPs	Weight loss (%)	Temperature (°C)	Inflection point
P-OTs	63.39	262.56 – 488.26	282
P-SAc	56.04	219.13 – 406.56	347
P-SH	50.14	291.08 – 454.55	341
P-SO_3H	43.30	230.03 – 493.82	342
P-OEt	39.64	312.55 – 656.23	416

4. Brunauer–Emmett–Teller (BET)

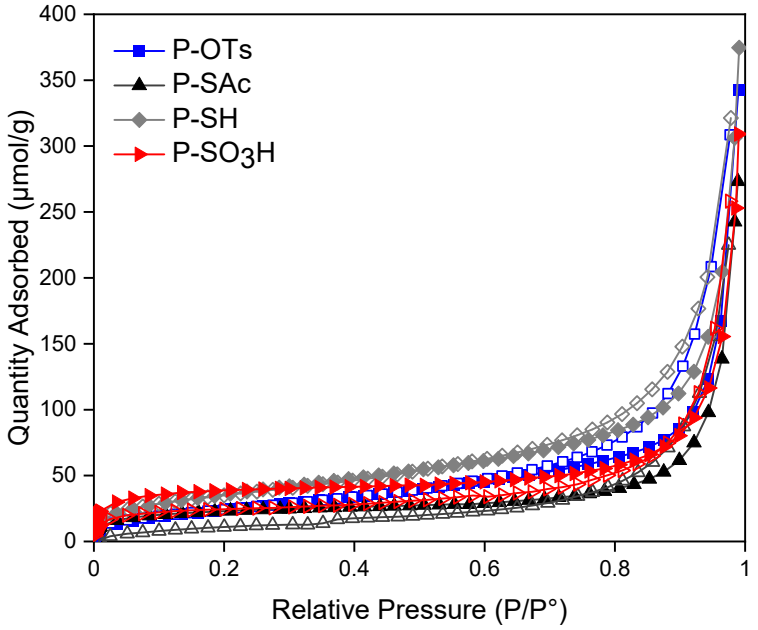

Figure S10 Nitrogen adsorption and desorption isotherms of sulfur functionalized HCPs (**P-OTs, P-SAc, P-SH, P-SO_3H)** at 77.3 K.

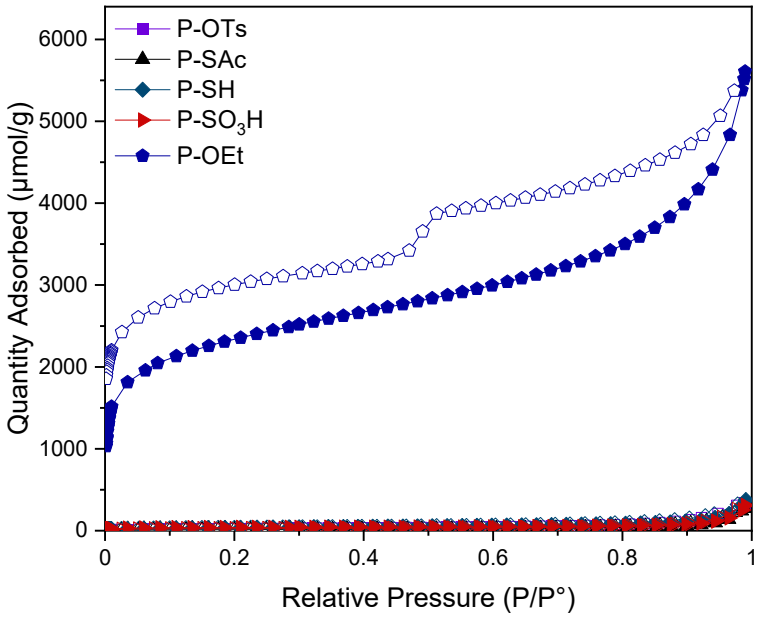

Figure S11 N_2 adsorption–desorption isotherms of **P-OTs, P-SAc, P-SH, P-SO_3H, P-OEt**

Table S4 Surface area and porosity of the sulphur-containing polymers.

Polymer	BET surface [a] (m^2g^{-1})	PV [b] (cm^3g^{-1})	PD [c] (Å)	Saturated adsorption [d] ($\mu mol\ g^{-1}$)
P-OTs	2.1588	0.004455	5.7710	160.056 ± 6.901
P-SAc	1.6900	0.002877	9.4810	10.728 ± 0.589
P-SH	3.0292	0.050100	7.2260	329.026 ± 14.988
P-SO_3H	2.6951	0.002986	11.9070	605.053 ± 27.396
P-OEt	169.8259	0.162806	12.3790	1439.429 ± 25.996

[a] Apparent surface areas calculated from nitrogen adsorption isotherms at 77.3 K using the BET equation. [b] Pore volumes calculated from the nitrogen isotherm at P/P0 = 0.995 and 77.3 K. [c] Adsorption average pore diameter (4V/A by BET). [d] Saturated adsorption calculated from Freundlich equation.

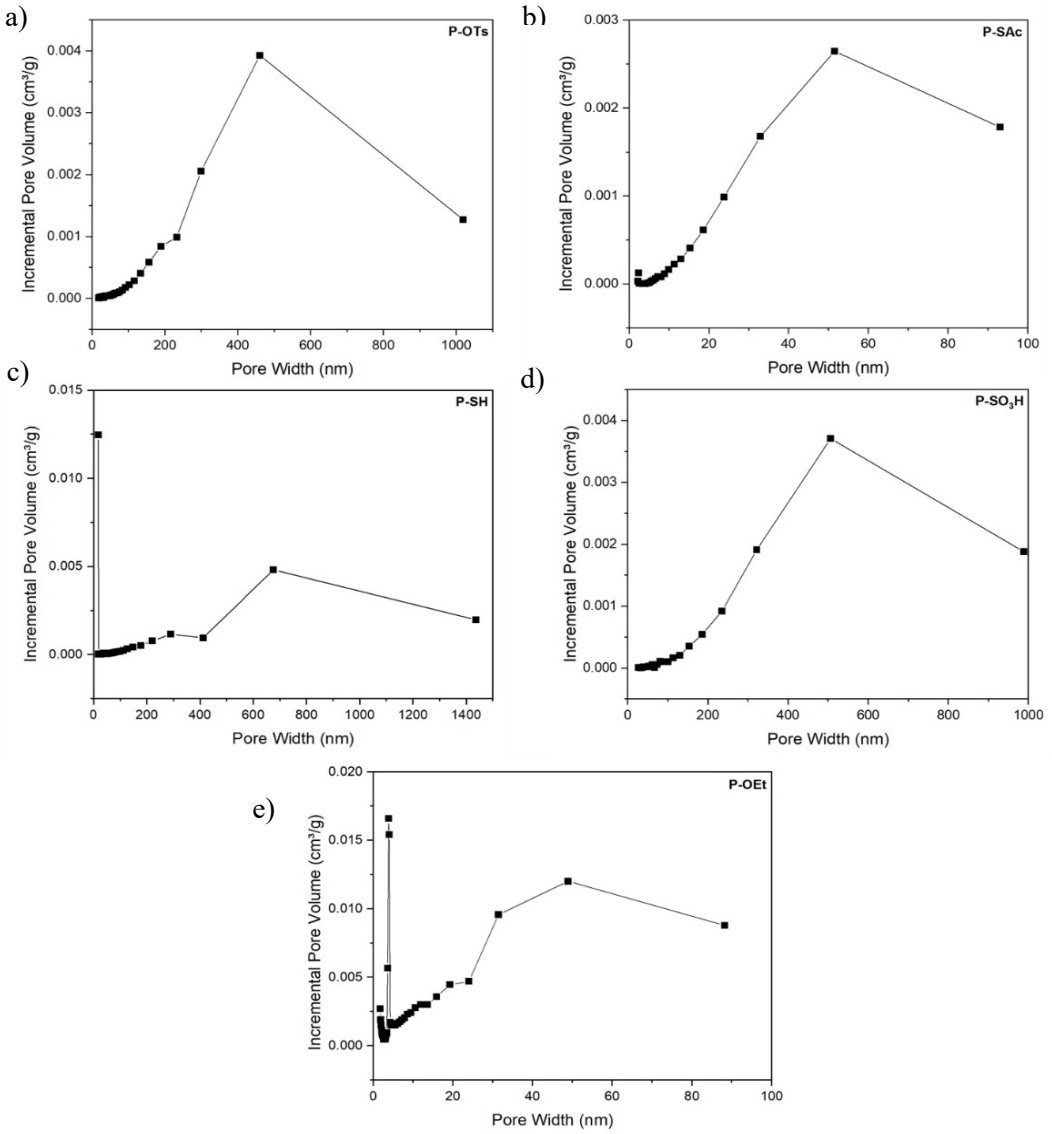

Figure S12 BJH pore size distribution derived from the desorption isotherm of (a) **P-OTs**, (b) **P-SAc**, (c) **P-SH**, (d) **P-SO_3H**, (E) **P-OEt**.

5. Scanning Electron Microscopy (SEM)

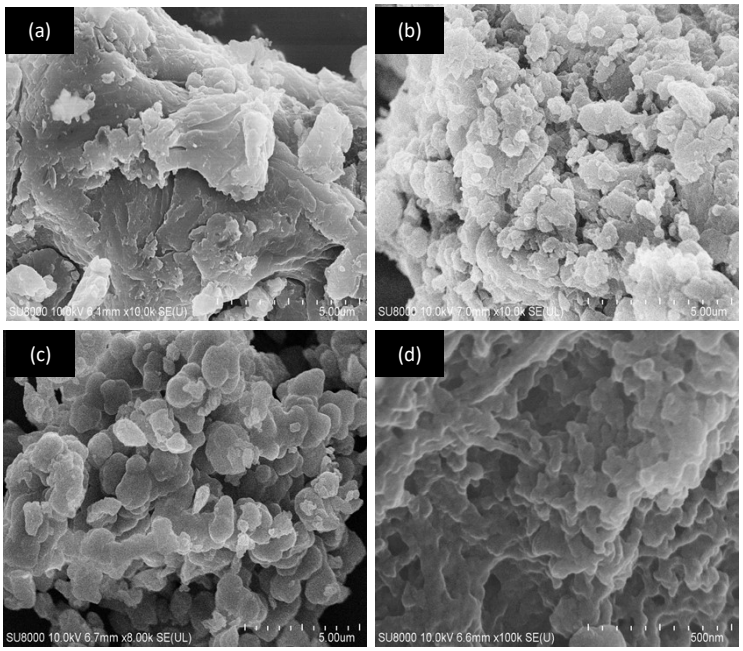

Figure S13 SEM images at high magnifications of (a) **P-OTs** (10K magnitude), (b) **P-SAc** (10K magnitude), (c) **P-SH** (8K magnitude), (d) P-**SO_3H** (100K magnitude)

Applications in organic pollutant removals from water

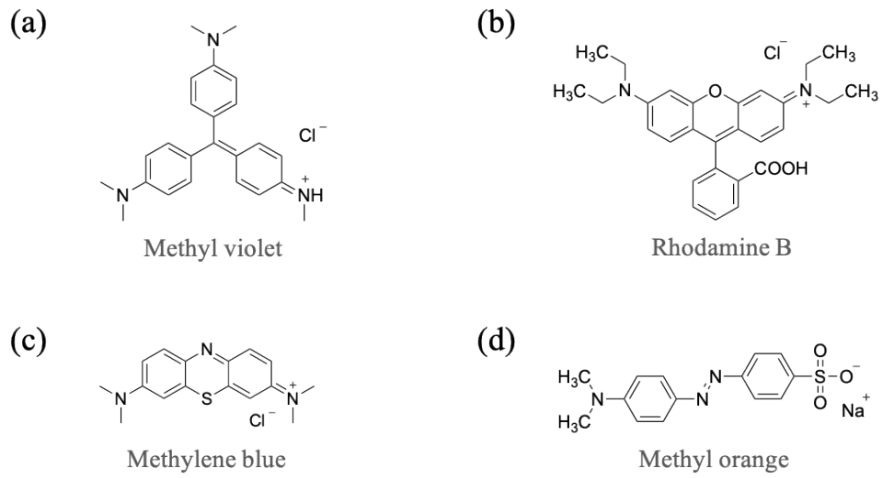

Figure S14 The chemical structures of organic dyes in this study

1. Adsorption selectivity of dyes on P-SO_3H

Table S5 adsorption selectivity of polymers in cationic dyes over anionic dyes

HCPs	MB:MO	RB:MO	MV:MO
P-OEt	0.8	0.7	1.1
P-OTs	1.5	1.0	0.9
P-SAc	5.7	2.7	8.8
P-SH	5.9	1.8	8.8
P-SO_3H	4.7	3.3	4.7

2. Kinetics

Table S6 Kinetic adsorption performance of paraquat and methylene blue in pseudo-first-order, pseudo-second order, and Intraparticle model.

Model	Concentration (mgL^{-1}) of PQ			Concentration (mgL^{-1}) of MB		
	100	**150**	**200**	**200**	**300**	**400**
pseudo-first-order						
q_e (mgg^{-1})	41.39	41.44	107.97	10.21	89.66	138.32
$k_{1\,(}$ min^{-1})	0.1955	0.4067	0.4090	0.3335	0.1538	0.1591
R^2	0.6697	0.7783	0.9372	0.5861	0.6779	0.8318
pseudo-second-order						
q_e (mgg^{-1})	90.99	142.45	193.80	199.20	277.78	400.00
h_o ($mgg^{-1}min^{-1}$)	134.22	1234.57	1063.83	3846.15	510.20	1351.35
k_2 ($gmg^{-1}min^{-1}$)	0.0162	0.0608	0.0283	0.0969	0.0066	0.0084
R^2	0.9999	1.0000	1.0000	1.0000	1.0000	1.0000
$t_{1/2}$ (min)	0.6779	0.1154	0.1822	0.0518	0.5444	0.2960
Intra-particle diffusion						
(mgg^{-1})	68.91	129.93	155.86	197.08	242.24	277.39
k_p ($mgg^{-1}min^{-1/2}$)	4.0225	2.5177	8.8441	0.6201	10.7640	29.8850
R^2	0.9358	0.6863	0.6951	0.3180	0.9510	0.8736

q_e: equilibrium adsorption capacity; k_1: pseudo-first-order rate constant; k_2: pseudo-second-order rate constant; k_p: Intraparticle diffusion rate constant; h_o: initial adsorption rate; c: boundary layer thickness constant; R^2: correlation coefficient.

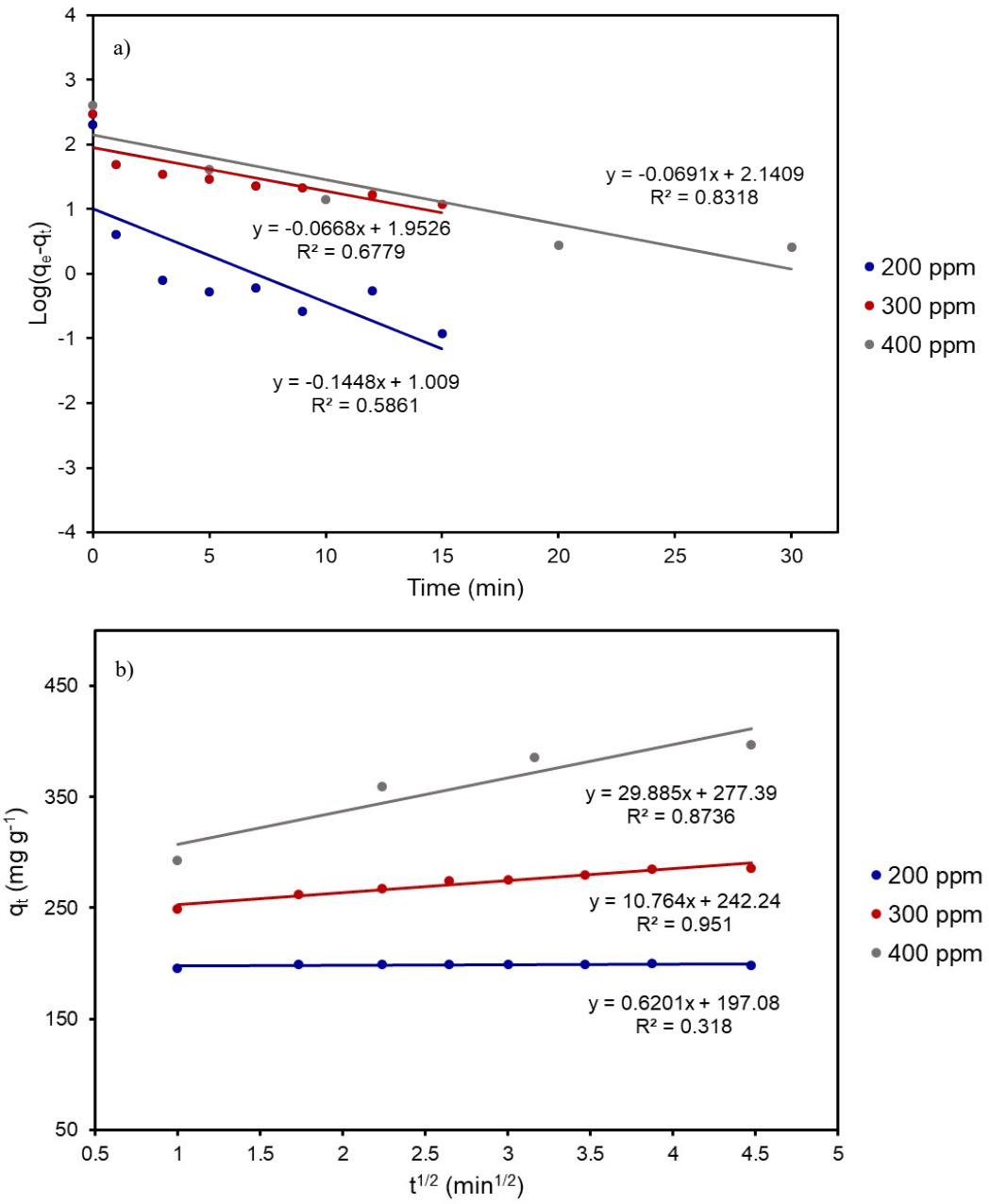

Figure S15 The realationship between $\log(q_e - q_t)$ and time according to pseudo-first-order adsorption model of MB (a), the realationship between q_t and $t^{1/2}$ according to the intra-particle diffusion model represented by the Webber-Morris (b).

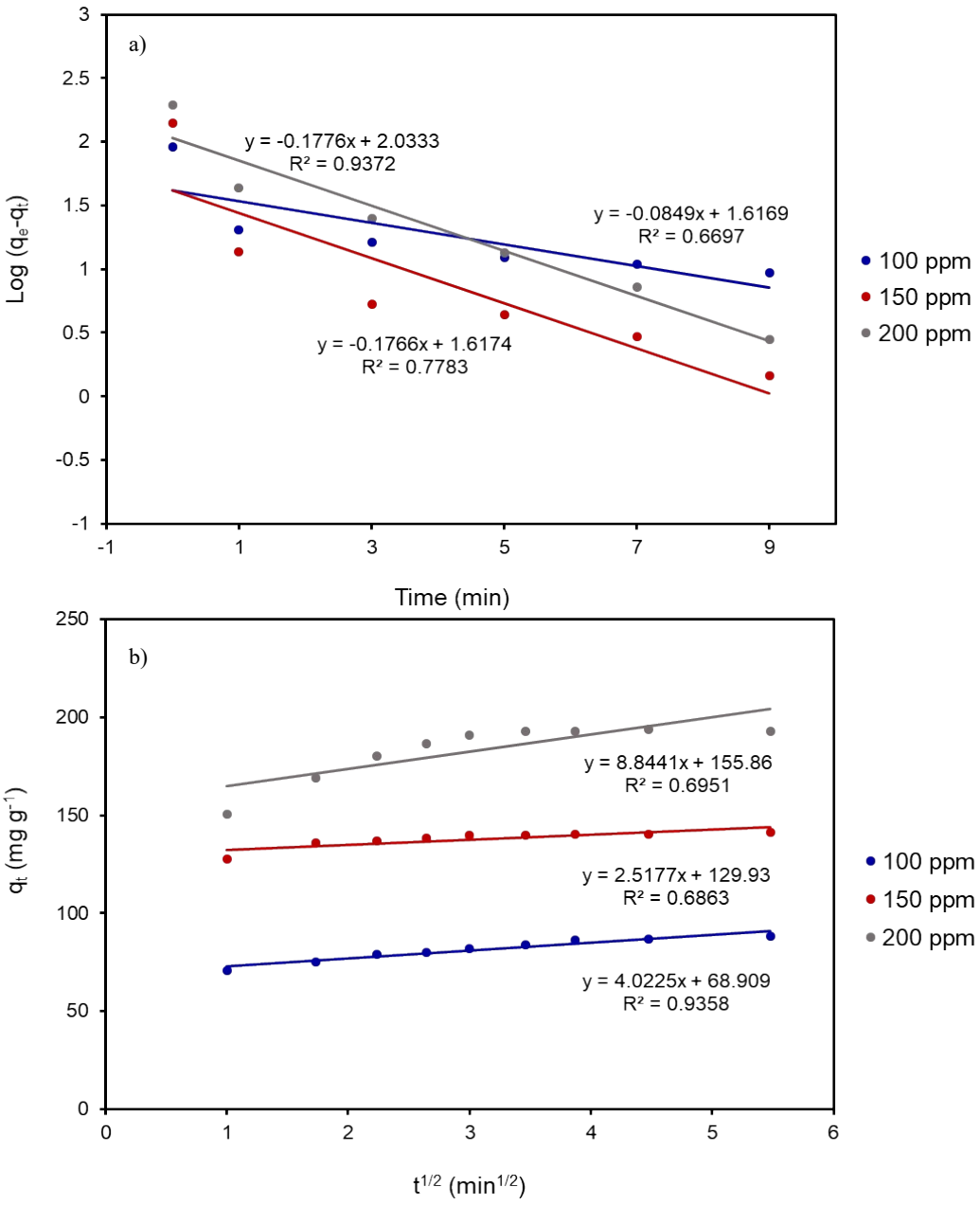

Figure S16 The realationship between log(q_e - q_t) and time according to pseudo-first-order adsorption model of PQ (a), the realationship between q_t and $t^{1/2}$ according to the intra-particle diffusion model represented by the Webber-Morris (b).

3. Adsorption isotherm

Adsorption Isotherm and Thermodynamics for the adsorption of **P-SO_3H** on organic pollutants. To study the adsorption isotherm and thermodynamics, 20 mg **P-SO_3H** was added into 40 mL centrifugal tube containing **PQ** or **MB** and kept in the water bath at a predetermined temperature (30 °C) for 2 h. The two models are the most commonly used including Langmuir (Equation S1), and Freundlich (Equation S2), followed by Dubinin–Radushkevich models (Equation S3), because the model parameters are simple and easy to interpretability.[2-5]

Langmuir equation:

$$\frac{C_e}{q_e} = \frac{1}{q_m K_L} + \frac{C_e}{q_m} \qquad \text{(S1)}$$

Freundlich equation:

$$\ln^{q_e} = \ln K_F + \frac{1}{n} \ln C_e \qquad \text{(S1)}$$

Dubinin–Radushkevich:

$$\ln q_e = \ln q_m - \beta\varepsilon^2 \qquad \text{(S3)}$$

where C_e (mgL^{-1}) is the equilibrium concentration of pollutants in solution; q_m (mgg^{-1}), the maximum adsorption capacity of the **P-SO_3H**; K_L (Lmg^{-1}), the Langmuir constant; K_F (Lg^{-1}), the Freundlich constant; 1/n gives information of the isotherm type: irreversible (1/n < 0), desirable (0 < 1/n < 1), undesirable (1/n > 1); β ($mol^2k^{-1}J^{-2}$), a constant related to the mean free energy of adsorption; and ε, the Polanyi potential, which is equal to RT ln(1 + (1/C_e)) (R (kJ/(mol K)) is the gas constant, T (K) is the temperature).

In addition, based on Langmuir model, it is essential to calculate the separation factor; R_L, which can be expressed in terms of a dimensionless constant and called the separation factor or equilibrium parameter. R_L can be defined as follows:

$$R_L = \frac{1}{1 + K_L C_1} \qquad \text{(S4)}$$

Where R_L is the separation factor and provides information on the adsorption process: unfavorable (RL > 1), favorable (RL < 1), linear (RL = 1), or irreversible (R_L= 0). C_1 (mgL^{-1}) is the highest initial pollutants concentration.

$$E = \frac{1}{\sqrt{2\beta}} \qquad \text{(S5)}$$

Based on the D−R model, E ($kJmol^{-1}$) is the free energy of the transfer of l mol adsorbate from solution to the adsorbent surface. It provides information about the adsorption type: physical ($E < 8\ kJmol^{-1}$) or chemical ($8\ kJmol^{-1} < E < 16\ kJmol^{-1}$).

Table S7 Parameters fitted by Langmuir, Freundlich and Harkins–Jura models (298 K).

Adsorption isotherm	Parameter	MB	PQ
	q_e ($mg \cdot g^{-1}$)	20000.00	943.40
Langmuir	K_L ($L \cdot g^{-1}$)	5.0340×10^5	1.5620×10^3
	R_L	0.9707	0.3903
	R^2	0.8716	0.9885
Freundlich	K_F ($mg^{1-1/n} \cdot (L^{1/n} \cdot g)^{-1}$)	1.2843	1.1609
	1/n	0.9496	0. 9596
	R^2	0.9902	0.9945
Dubinin-Radushkevich	q_m($mg \cdot g^{-1}$)	423.34	319.50
	β	2449.16	852.78
	E ($kJ\ mol^{-1}$)	0.0143	0.0242
	R^2	0.8054	0.6236

4. The effect of pH in adsorption performance

a) b)

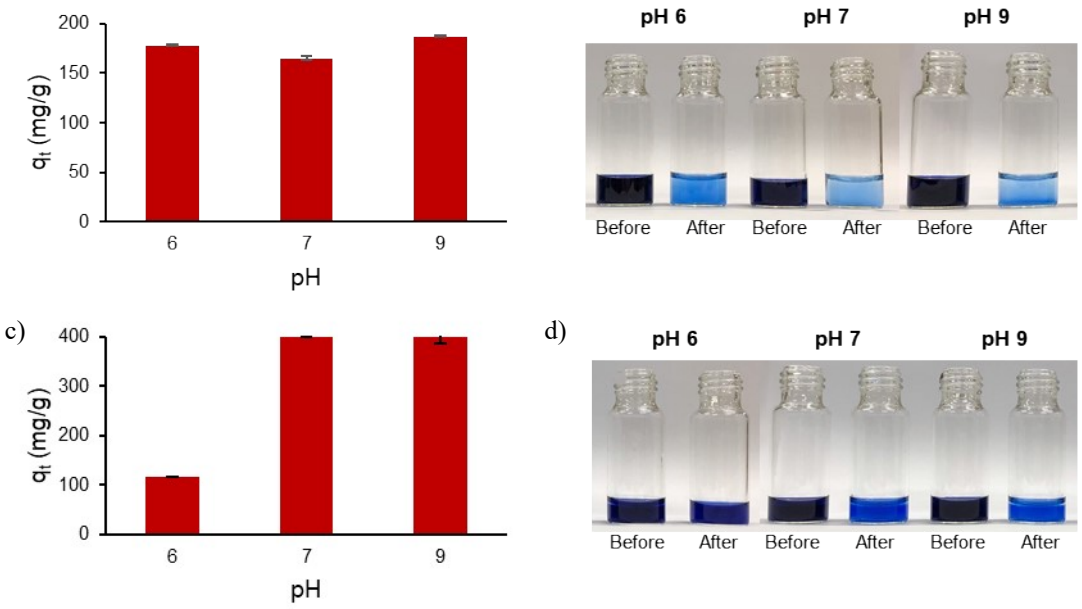

Figure S17 The adsorption performance of **P-SO_3H** in pH 6, 7, and 9 for (a-b) PQ, (c-d) MB.

5. The effect of common ions in solution and ionic strength of solution

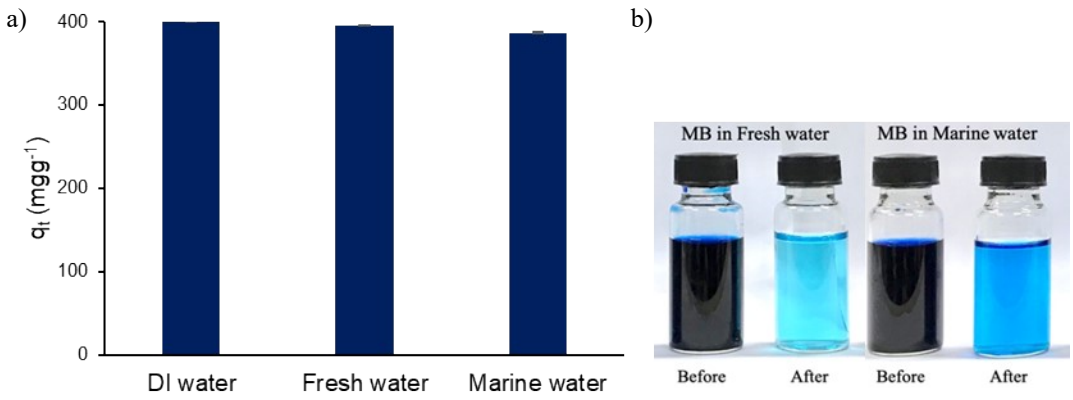

Figure S18 (a) Adsorption profile of MB in DI water, artificial freshwater, and artificial seawater by **P-SO_3H**, (b) Photograph of MB before and after adsorption process.

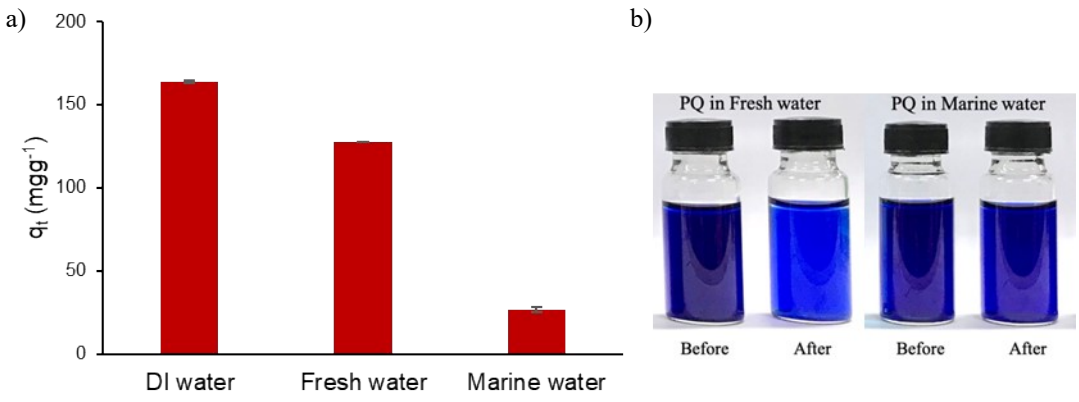

Figure S19 (a) Adsorption profile of **PQ** in DI water, artificial freshwater, and artificial seawater by **P-SO$_3$H**, (b) Photograph of **PQ** before and after adsorption process.

6. Reusability

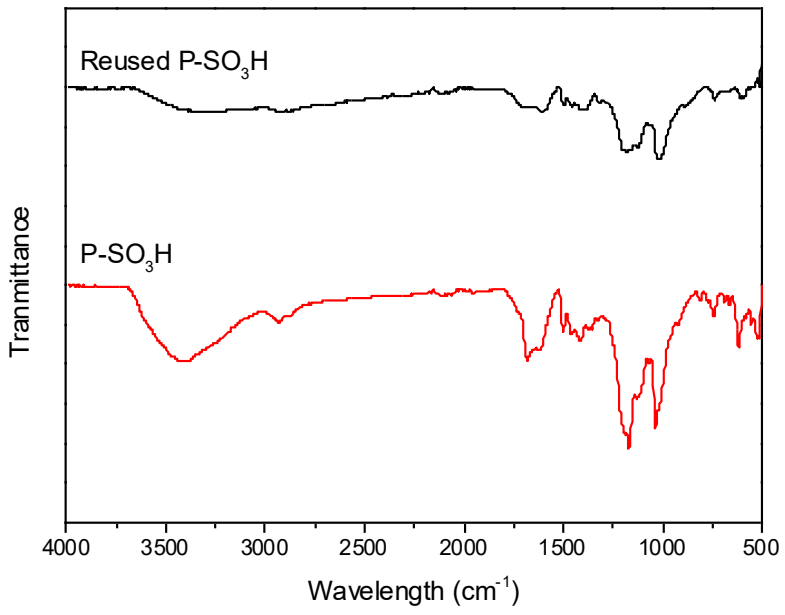

Figure S20 IR spectra of **P-SO_3H** before adsorption process and after reusability of 7 cycles.

References

1. Guijarro, E. C.; Yáñez-Sedeño, P.; Diéz, L. M. P., Determination of paraquat by flow-injection spectrophotometry. *Anal. Chim. Acta* **1987,** *199*, 203-208.
2. Langmuir, I., THE ADSORPTION OF GASES ON PLANE SURFACES OF GLASS, MICA AND PLATINUM. *J. Am. Chem. Soc.* **1918,** *40* (9), 1361-1403.
3. Hall, K. R.; Eagleton, L. C.; Acrivos, A.; Vermeulen, T., Pore- and Solid-Diffusion Kinetics in Fixed-Bed Adsorption under Constant-Pattern Conditions. *Industrial & Engineering Chemistry Fundamentals* **1966,** *5* (2), 212-223.
4. Dubinin, M. M.; Radushkevich, L. V., The Equation of the Characteristic Curve of Activated Charcoal. *Proc. acad. sci. USSR. Phys. chem. sect.* **1947,** *55*, 331.
5. Freundlich, H. M., Over the Adsorption in Solution. *J. Phys. Chem.* **1906,** *57*, 385-471.